

AperTO - Archivio Istituzionale Open Access dell'Università di Torino

Variable membrane protein A of flavescence dorée phytoplasma binds the midgut perimicrovillar membrane of *Euscelidius variegatus* and promotes adhesion to its epithelial cells

This is the author's manuscript

Original Citation:

Availability:

This version is available <http://hdl.handle.net/2318/1668948> since 2018-05-24T15:32:47Z

Published version:

DOI:10.1128/AEM.02487-17.

Terms of use:

Open Access

Anyone can freely access the full text of works made available as "Open Access". Works made available under a Creative Commons license can be used according to the terms and conditions of said license. Use of all other works requires consent of the right holder (author or publisher) if not exempted from copyright protection by the applicable law.

(Article begins on next page)

Variable membrane protein A of flavescence dorée phytoplasma binds the midgut perimicrovillar membrane of *Euscelidius variegatus* and promotes adhesion to its epithelial cells

Running title: Phytoplasma adhesion to insect vector cells

Nathalie Arricau-Bouvery^{1#}, Sybille Duret¹, Marie-Pierre Dubrana¹, Brigitte Batailler¹, Delphine Desqué¹, Laure Béven¹, Jean-Luc Danet¹, Michela Monticone², Domenico Bosco², Sylvie Malembic-Maher¹, and Xavier Foissac¹

¹ INRA, Univ. Bordeaux, UMR 1332 de Biologie du Fruit et Pathologie, CS20032, 33882, Villenave d'Ornon Cedex, France

² Università di Torino, DISAFA – Entomologia, Largo Paolo Braccini, 2, 10095 Grugliasco (TO), Italy

[#] Corresponding author: Nathalie Arricau-Bouvery, nathalie.bouvery@inra.fr

Abstract

Phytoplasmas are uncultivated plant pathogens and cell wall-less bacteria and are transmitted from plant to plant by hemipteran insects. Phytoplasmas' circulative propagative cycle in insects requires the crossing of the midgut and salivary glands, and primary adhesion to cells is an initial step towards the invasion process. The flavescente dorée phytoplasma possesses a set of variable membrane proteins (VmPs) exposed to its surface, and this pathogen is suspected to interact with insect cells. The results showed that VmpA is expressed by the flavescente dorée phytoplasma present in the midgut and salivary glands. Phytoplasmas cannot be cultivated at present, and no mutant can be produced to investigate the putative role of VmPs in the adhesion of phytoplasma to insect cells. To overcome this difficulty, we engineered the *Spiroplasma citri* mutant G/6, which lacks the adhesins ScARPs, for VmpA expression and used VmpA-coated fluorescent beads to determine if VmpA acts as an adhesin in *ex vivo* adhesion assays and *in vivo* ingestion assays. VmpA specifically interacted with *Euscelidius variegatus* insect cells in culture and promoted the retention of VmpA-coated beads to the midgut of *E. variegatus*. In this latest case, VmpA-coated fluorescent beads were localized and embedded in the perimicrovillar membrane of the insect midgut. Thus, VmpA functions as an adhesin that could be essential in the colonization of the insect by the FD phytoplasmas.

Importance

Phytoplasmas infect a wide variety of plants, ranging from wild plants to cultivated species, and are transmitted by different leafhoppers, planthoppers and psyllids. The specificity of the phytoplasma-insect vector interaction has a major impact on the phytoplasma plant host range. As entry into insect cells is an obligate process for phytoplasma transmission, the bacterial adhesion to insect cells is a key step. Thus, studying surface-exposed proteins of phytoplasma will help to identify the adhesins implicated in the specific recognition of insect

vectors. In this study, it is shown that the membrane protein VmpA of the flavescence dorée phytoplasma acts as an adhesin that is able to interact with cells of *Euscelidius variegatus*, the experimental vector of the FD phytoplasma.

INTRODUCTION

Phytoplasmas are bacteria responsible for diverse epidemic diseases in various cultivated and ornamental plants (1, 2). Characterized by the absence of a cell wall and no peculiar morphology, they belong to the class *Mollicutes* in the order *Acholeplasmatales*, “*Candidatus* genus Phytoplasma”. These bacteria are exclusively located in the sieve elements of plant hosts and are propagated by numerous insect vectors from the Order Hemiptera (3). In hosts, plants and insects, phytoplasmas are found intracellularly. In insects, these bacteria colonize different organs, such as the intestinal tract, muscles and salivary glands (4). Phytoplasma members of the 16SrV-C and V-D taxonomic subgroups cause a severe epidemic disease of grapevine called flavescence dorée (FD) and have therefore been classified as quarantine pests. These phytoplasmas are propagated within and from vineyard to vineyard by the Deltocephalinae leafhopper *Scaphoideus titanus* Ball (5), which was introduced in France well before 1950 (6). These grapevine-specialized insects, from the first nymphal to imago stages (7), acquire phytoplasmas while feeding on infected grapevines and subsequently become infectious after a latency period. The use of insecticide treatments against the vector is one of three main ways to control flavescence dorée, with the other two being planting phytoplasma-free material for planting and removing infected grapes. However, chemical treatments cause unwanted economic, social and environmental impacts and must be reduced. To strengthen such an improvement in FD management, a better

understanding of the mechanisms leading to phytoplasma transmission, especially the acquisition phase, is necessary.

In the insect vector, the cycle is persistent and multiplicative (8). This property implies the crossing of the two barriers represented by the intestine epithelium and the salivary gland cells but also the multiplication of bacteria into insects. Phytoplasmas have the capacity to multiply into a wide variety of cellular types, such as the intestine, particularly the muscle layer of the midgut, and salivary glands (9, 10), but FD phytoplasmas have not been detected in the sexual organs (11). Passing through intestinal and salivary gland cells is clearly mediated by endocytosis; next, there is movement into the cytoplasm and then exocytosis, as is the case for *Spiroplasma citri*, another plant pathogen of the class *Mollicute* transmitted by leafhoppers (12, 13). These steps imply the direct interactions between phytoplasma and eukaryotic cell proteins to promote endocytosis by cells that are not specialized in phagocytosis. Lacking specialized organelles for mobility or kinetic cytoskeleton, phytoplasmas have to move from apical to basal membranes and leave the host cell by exocytosis after multiplication. All of these steps must be achieved without altering tissue integrity to avoid toxicity to their vector. Several genomes of “*Ca. Phytoplasma*” species are available from which proteins that are predicted to be secreted or surface-exposed are tentatively selected for functional studies. However, notably few protein functional studies have been described in relation with insect transmission. Among the three types of immunodominant membrane proteins (IDPs) that are the major membrane proteins of phytoplasmas (14), the Amp of “*Ca. P. asteris*” was observed to interact with the three main proteins of the microfilament complex, *i.e.*, the actin and myosin light and heavy chains of the intestinal smooth muscle, as well as with the ATP synthase of leafhopper vector (15, 16). Although Amp is essential for transmission by insect vectors (17), Amp interacts with insect proteins after phytoplasmas have become intracellular and could be implicated in the

movement of phytoplasmas across these cells. However, phytoplasma adhesins, which are necessary for the promotion of the adhesion of phytoplasma to cells in the digestive tract and salivary glands, have not been identified to date. Several immunogenic membrane proteins that are present at the surface of the phytoplasmas, such as the variable membrane protein Vmp1 of “*Ca. P. solani*”, are targets of strong selective pressures (18). This finding suggests the proteins’ implication in interactions with host molecules. VmpA, similar to Vmp1, is a variable membrane protein predicted to be destined to the FD phytoplasma (FD-P) surface by the Sec-dependent pathway to be finally anchored to the membrane by a C-term transmembrane segment (19). Several other genes found in the genome of the FD-P encode variable membrane proteins, including VmpB, which share the same structure (20). The structure of FD-P VmpA also contains a hydrophilic central that possesses 3 complete repeats of 78 amino acids exposed to the phytoplasma surface. This finding is consistent with the possible role of VmpA in the FD-P adhesion to insect cells, as repeated domains are commonly found in bacterial proteins involved in cell recognition (21). Such adhesins have been characterized in *S. citri* (22–24), and in *Mycoplasma agalactiae* (25, 26). Thus, the role of VmpA in the adhesion of the phytoplasma to insect cells was examined.

The *in vitro* culture of leafhopper vector cells provides an experimental tool to study the phytoplasma-insect interaction at the cellular level. For example, it had been demonstrated that the ability of *S. citri* to invade insect cells *ex vivo* is correlated to its ability to be transmitted by the leafhopper vector *Circulifer haematoceps* (27). Additionally, a useful experimental cycle was done to transmit FD-P to the broad bean *Vicia faba* using the leafhopper *Euscelidius variegatus* (28), which similar to *S. titanus*, belongs to the Deltocephalinae subfamily. This prompted us to use cultured cells of *E. variegatus* to explore the implication of the strain FD92 (FD92-P) VmpA in the adhesion process of FD-P to insect cells. In this study, antibodies were used to ascertain the VmpA expression by FD92-P in the

insect *E. variegatus*, and we measured the adhesion to *E. variegatus* cells of recombinant spiropasmas expressing VmpA and fluorescent latex beads coated with His₆-tagged VmpA. The interaction of VmpA-His₆-coated beads with the apical surface of midgut epithelial cells was assessed in *in vivo* ingestion assays.

RESULTS

1- VmpA protein is expressed by FD92 phytoplasmas in insects

To assess VmpA expression by FD92-P in the intestinal tract and the salivary glands, indirect immunofluorescence labeling and confocal observations were used. VmpA proteins were visualized in the phytoplasmas in midguts 2 weeks after feeding acquisition with infected broad beans, and they were still detected five weeks after infection (Fig 1). Bacteria were located in intestine cells (arrows), and a number were observed considerably closer to actin filaments of the muscle fibers covering the basal lamina (arrowheads). VmpA was also detected in the salivary glands of some insects, already two weeks after feeding acquisition (Fig 2) and in the majority of insects after a longer latency period of 4 and 5 weeks (Fig 2). No labeling was observed in the midgut and salivary glands of healthy insects. The detection of VmpA by immuno-labeling showed that the FD92-P infecting *E. variegatus* produced VmpA both in the midgut and salivary glands.

2- Euva-1 cell line

A cell line from *E. variegatus* was established to study the cellular and molecular interactions between phytoplasma proteins and insect cells. Ten months of the continuous culturing of cells isolated from embryos of *E. variegatus* resulted in the Euva-1 cell line. Cell morphology was examined by light microscopy using methylene blue staining and the

fluorescent labeling of actin filaments and nuclei. Based on cellular morphology and colorations, the Euva-1 cell line possessed three main cellular types. The first cells were the largest ones and had only their nucleus stained with methylene blue (Fig. 3, asterisk). The second cell type had its nucleus and cytosol colored (Fig. 3, arrow), while the third was the smallest in size and was darker colored by methylene blue (Fig. 3, arrowhead). Actin coloration showed that the type 2 and 3 cells had clear attachment fibers and filopodia, enabling them to adhere to the flask (Fig. 3B). The two first cell types resembled epithelial cells, whereas the nature of the third was unknown. The interaction experiments were performed with cells cultivated between passages 15 and 21.

The sequencing of the mitochondrial marker cytochrome oxidase subunit I (COI) was used to confirm the leafhopper origin of the Euva-1 cell line. Sequences from the mitochondrial marker amplified from Euva-1 cell DNA and from the *E. variegatus* insect DNA were found to be identical (data not shown). A BLAST search in the GenBank database revealed that this sequence shared 80% nucleotide identity with the COI gene of the Cicadellinae *Acrogonia virescens*, which may be its closest relative.

3- VmpA-coated beads adhere to *E. variegatus* leafhopper cells in culture

As a phytoplasma mutant cannot be engineered at present, we used recombinant VmpA proteins to test the interaction between VmpA and the insect cells *ex vivo*. For that purpose, we covalently linked VmpA-His₆ recombinant protein and GFP, which served as negative control, to NH₂-beads instead of COOH-beads to better mimic the surface exposition of the VmpA N-terminal part. In these adherence assays, fluorescent beads were incubated for 1 h with Euva-1 cells and counted by epifluorescence observation (Fig 4A). The adhesion of beads to Euva-1 cells significantly augmented with increasing concentrations of VmpA, and

the median number of adherent beads was 3-fold higher when beads were linked with 9 nmol of VmpA than the control beads coated with GFP only (Fig 4B).

To evaluate the specificity of VmpA adhesion to insect cells, we used competitive and inhibition adhesion assays. The adhesion of the fluorescent VmpA-His₆-coated beads was strongly decreased in the presence of anti-His₆-VmpA antibodies (PAb) in a dose-dependent manner (Fig. 4C), although a small but significant increase of bead adhesion was measured when few antibodies were used (1/1000 dilution). When anti-spiraline PABs were used as a negative baseline control, as expected, the adhesion rate was not significantly changed. No visible aggregation of the VmpA-His₆-coated beads was observed in the presence of anti-His₆-VmpA PABs (data not shown). The results of competitive adhesion assays show that the presence of an increasing quantity of His₆-VmpA overlaying the leafhopper cells decreased the adhesion of VmpA-His₆-coated beads in a concentration-dependent manner (Fig. 4D). In parallel experiments, we used the other predicted surface-exposed protein VmpB, which is also expressed in the insect *E. variegatus* (Fig. S1). No reduction was observed when the cells were pre-incubated with the His₆-VmpB recombinant protein. Taken together, these results strongly suggest that VmpA was able to specifically interact *in vitro* with the cells of the FD-P experimental insect vector *E. variegatus*, as an adhesin would do.

4- VmpA allows the adhesion of recombinant *S. citri* to leafhopper cells in culture

To complete functional studies on phytoplasma proteins, spiroplasmas that express VmpA at their surface were engineered to measure the impact of VmpA on bacterial adhesion to insect cells (19). We first verified that the recombinant *S. citri* G/6 strain still produced the protein VmpA after several passages before the adhesion assay. A comparison of VmpA expression in recombinant *S. citri* was conducted in the presence and absence of antibiotic selection pressures to promote the stability of pSTVA1. Two clones of *S. citri* G/6 carrying

pSTVA1 (clones 5 and 6) were plated on SP4 agar, and different sub-clones were cultivated for 5 passages. The pSTVA1 plasmid was easily detected in the presence of tetracycline, while in the absence of the antibiotic, it was visualized in the sub-clone 6g only, but the restriction map was incorrect, suggesting a deletion (Figure 5A). Thus, PCR amplifications and sequencing were performed to verify the presence of a correct *vmpA* sequence. In the case of sub-clone 6g, a deletion of approximately 700 bp was observed, corresponding to the size of the repeat domains that contain the VmpA protein, and confirmed the plasmid profile after *HindIII* restriction. In the case of the sub-clones 5e and 5h, amplicons were observed after electrophoresis, which suggests that pSTVA1 plasmids were present in these two sub-clones. No deletion or mutation in the *vmpA* gene was observed in clones propagated in the presence of the antibiotic and in the sub-clones 5e and 5h propagated without the antibiotic. When the expression of VmpA was monitored by Western blot (Figure 5A), differences in VmpA expression were observed between spiroplasmas cultivated in the presence or absence of tetracycline. When the antibiotic was omitted, the production of VmpA was abolished. In contrast, the culture of the sub-clones in the presence of tetracycline allowed for the strong detection of VmpA. Thus, second culture passage of recombinant *S. citri* was performed only in the presence of tetracycline for adhesion assays, and the production of VmpA was verified by colony blot.

Adhesion assays were performed by comparing the *S. citri* G/6 strain carrying the plasmid pSTP2 (vector without *vmpA*) to G/6 carrying pSTVA1. The colony blots showed that 50 to 100% of the spiroplasmal colonies were expressing VmpA, depending on the replicates, and as revealed by immunoblot. A significant increase of adhesion was observed when VmpA was expressed by the recombinant spiroplasmas (Fig 5B). These results reinforce the previous results to show that VmpA acted as an adhesin binding to Euva-1 cells.

5- Interaction of VmpA with the midgut

To assess the role of VmpA in the adhesion of phytoplasmas to intestinal epithelial cells, we used fluorescent beads to localize and count the VmpA-His₆-coated beads in the midguts of *E. variegatus* in *in vivo* experiments. After ingestion by insects, the fluorescent latex beads were only observed in the midgut and occasionally in the filter chamber but were never detected in the Malpighian tubules (Fig. 6A). A high variability of the number of retained beads could be observed between insects (Fig. 6B), but it was reproducible among 3 independent experiments. Regardless of the amount of VmpA-His₆ bound to the fluorospheres, the number of beads per surface unit was observed to be higher in the anterior midgut compared to the middle midgut. Furthermore, the higher the quantity of VmpA-His₆ coupled to the beads, the greater amount of beads was attached to the midgut surface. When VmpA was in excess compared to BSA, the beads attached to the anterior midgut were too numerous to be accurately quantified. For this reason, counting was performed only at the middle midgut level. As shown in figure 6B, VmpA-His₆-coated fluorescent beads were more greatly retained in midguts than BSA-coated beads did at one, two and four days after feeding acquisition. Seven days post-ingestion, the number of VmpA-His₆-coated beads fell and showed values similar to those of BSA-coated beads four days after ingestion. These results suggest that VmpA, unlike BSA, is more strongly retained in the luminal surface of midgut cells.

6- VmpA-His₆-coated beads are localized and embedded in the perimicrovillar membrane of midguts

To more precisely localize the VmpA-His₆-coated beads in the midgut at the cellular level, we used transmission electron microscopy (TEM). Midguts dissected from leafhoppers that had ingested VmpA-His₆-coated beads in HEPES-sucrose for two days and then having

fed healthy broad bean for one day were compared to leafhoppers that were only fed healthy broad bean (Fig. 7). Bacteria-like particles were visualized in the lumen of the midgut and in the anterior and middle midgut of insects, regardless of whether the leafhoppers were fed (Fig. 7, arrowheads). The particles were often associated with a structure that resembles the perimicrovillar membrane in the anterior and medium parts of midgut. In the midgut of insects that had ingested beads coated with VmpA-His₆, the beads were clearly visible in the lumen (asterisks in Fig. 7B and 7C). The beads were found alone or in groups, embedded in the perimicrovillar membrane, and certain beads were clearly in contact with the microvilli of epithelial cells (Fig. 7C, arrow). In the anterior part of the midgut, the VmpA-His₆-coated beads were present in a larger quantity than in the medium midgut, as previously observed by fluorescence microscopy. Beads were observed in the same gut lumen section where bacteria-like particles were also visualized. No beads were seen inside cells, regardless of where the observation was conducted. Other small dense unidentified particles could also be seen within epithelial cells. As a control, microscopy observations did not show differences between leafhoppers having been fed HEPES-sucrose or healthy broad bean (data not shown). Taken together, TEM observations suggest an affinity of VmpA for the perimicrovillar membrane that covers the apical surface of epithelial cells.

DISCUSSION

Because phytoplasmas have not been cultivated *in vitro* to date, no defective mutants are available to study candidate genes putatively implicated in phytoplasma adhesion to insect cells. Fortunately, *Spiroplasma citri*, another plant pathogen also transmitted by Cicadellidae insects, is amenable to genetic manipulation. The *S. citri* GII3 mutant G/6, devoid of the adhesins ScARPs (24, 29), was transformed to express the VmpA protein of the FD-P strain

266 FD92 at the spiroplasmal surface (19). We used the mutant *S. citri* G/6, as it is deficient for
267 the adhesion to insect cells (24), to express VmpA with the aim of increasing the spiroplasmal
268 adhesion to the *E. variegatus* cells. To screen the adhesion-like properties of phytoplasma
269 surface proteins, the recipient cell line Euva-1 was established from the experimental vector
270 *E. variegatus* of the FD92 phytoplasmas. The percentages of Euva-1 cells with adherent
271 spiroplasmas G/6 measured in this study were low and similar to those observed when this
272 defective strain was incubated with Ciha-1 cells, a cell line derived from one of *S. citri* natural
273 vectors, *Circulifer haematoceps* (24). The expression of VmpA at the surface of this G/6
274 mutant resulted in recombinant spiroplasmas to significantly increase their adhesion to Euva-1
275 cells. These results are reinforced by experiments that show an enhanced adhesion of VmpA-
276 coated fluorescent beads to the same cells. Taken together, these data demonstrate that VmpA
277 acts as an adhesin, regardless of the support used. Thus, *S. citri* was confirmed to be a good
278 model to functionally characterize adhesins or other surface proteins of phytoplasmas. By
279 extension, it should constitute a reliable experimental platform for the simultaneous
280 expression of sets of phytoplasma proteins acting in concert in the adhesion and entry
281 phenomenon. However, the results also indicated that an antibiotic pressure was necessary to
282 maintain the VmpA expression encoded by the pSTVA1 plasmid. The pSTVA1 plasmid is a
283 derivative of the plasmid pSci21NT, a modified-pSci natural plasmid of *S. citri* GII3 (19), and
284 it was stably expressed in the non-transmissible *S. citri* strain 44 (30). The plasmids pScis are
285 present in 10 to 14 copies per cell (31), which might also be the case for pSci derivatives. The
286 instability of pSTVA1 could therefore result from an increase in the metabolic energy
287 necessary for plasmid maintenance and function or from the general deleterious effect on the
288 bacterial growth rate (32, 33). There are many reports that show that overexpressed
289 heterologous membrane proteins can affect the bacterial growth rate by imposing a metabolic
290 burden, an overload of the membrane biogenesis machinery, a membrane stress or local

membrane disruptions in bacteria (33–35). Thus, one possible explanation for the lack of VmpA detection in the absence of tetracycline is that expression of this protein decreases *S. citri* fitness and produces counter selection, leading to the loss of VmpA expression. Such instability of viral-derived vector has previously been observed for *S. citri* viral vectors engineered to express a fragment of a mycoplasma adhesin (35).

As shown in the current paper, phytoplasmas expressing VmpA were observed in the intestinal cells of *E. variegatus*, a necessary condition to envisage its role in the adhesion to intestine cells. In addition, the ingested VmpA-His₆-coated beads were more greatly retained in the midgut than those predominantly coated with BSA, especially when the beads were coated with a higher amount of VmpA. This validates the hypothesis that VmpA could play a major role in midgut colonization. Ingested coated beads have been observed to be embedded in a matrix associated with the apical surface of microvilli, occasionally with bacteria in the anterior midgut. One of these bacteria might be the congenitally-transmitted enterobacterium previously observed by Cheung and Purcell (36, 37). The bead location was similar to that of maize bushy stunt phytoplasma cells in the midgut lumen of *Dalbulus maidis* (37). Packed maize bushy stunt phytoplasmas were observed by the authors in the lumen near the microvilli and appeared to be surrounded by a slightly electron-dense structure resembling the structure in which the VmpA-coated beads were detected. The precise composition of the *E. variegatus* matrix observed in the lumen of *E. variegatus* since 1993 has not been deciphered to date (36). In our observations, the size of this structure is similar to that observed by these authors and is approximately 2-6 μm wide. This matrix had been called glycocalyx by Cheung and Purcell, but according to recent studies on hemipteran insects, we prefer calling it perimicrovillar membrane (39). Unlike lepidopterans and coleopterans, euhemipterans lack a peritrophic membrane (PM). Their perimicrovillar membrane (PMM) is partly composed of glycoproteins (40). In euhemipterans, this PMM seems to act as a protective barrier against

invasive microbes and could have diverse functions in the digestion and absorption of nutrients. Microorganisms blocked by the PMM and that use adhesins to stick to the PMM and escape the feeding bowl flow must cross through to reach the apical surface of gut epithelial cells to finally undergo midgut colonization. One example is *Trypanosoma cruzi*, which is attached to the PMM of the Chagas disease vector bug *Rhoniis prolixus*. This attachment is mediated via lectin-like proteins of *T. cruzi* to glycoproteins of the midgut PMM (42). Similar to the surface lectin spiralin of *S. citri* (43, 44), VmpA enables *S. citri* and fluorescent beads to adhere to insect cells in culture and to the PMM, which is rich in glycoconjugates. VmpA has also been detected on phytoplasmas attached to the salivary glands, the surface of which is glycosylated like the different lobes of *Circulifer haematoceps* salivary glands (41). Because of these analogies between the two models, a lectin activity for VmpA could therefore be hypothesized and should be further investigated. In the case of another pathosystem, the TnGV granulosis virus encodes the metalloprotease enhancin that alters the structural integrity and porosity of the lepidopteran PM and results in an increased movement of the virus (43). Regarding the structural and functional domains found in VmpA, a PepSY motif that is implicated in regulation of peptidase activity (44) was found upon *in silico* analysis. In this regard, VmpA could promote the local degradation of the PMM protein component, allowing phytoplasmas to reach the apical membrane of the midgut epithelium. Nevertheless, these two VmpA activities remained to be investigated.

During their cycle within their vectors, phytoplasmas have to invade diverse types of cells or different vectoring insects. These successive steps must involve different phytoplasma membrane-associated proteins, as this has been deciphered in the *Spiroplasma* models (22, 24, 41, 42, 45). In the case of FD92-P, VmpB, which shows a similar structure, is a potential candidate to have a similar function. Competition adhesion assays showed that VmpB does not inhibit the adhesion of VmpA to insect cells, suggesting that if VmpB interacts with insect

proteins, it is probably not targeting the same receptor(s). The recent deciphering of the FD92-P (20) chromosome will help to compile the list of the potential actors in phytoplasma-insect vector interactions. The use of the Euva-1 cells and recombinant spiroplasmas should be of great help in addressing this challenge.

MATERIALS AND METHODS

Insects, bacterial strains and culture conditions

Phytoplasma-free *Euscelidius variegatus* leafhoppers were reared in cages on broad bean (*Vicia faba* var. aquadulce) and oat (*Avena sativa*) at 25°C. The phytoplasma strain FD92 (FD92-P) was originally transmitted to broad bean (*Vicia faba* var. aquadulce) by infected *Scaphoideus titanus* sampled on FD-diseased vineyards in southwest France (46, 47) and was continuously maintained in broad bean by *Euscelidius variegatus* transmissions as described by Caudwell and colleagues (48).

The *Spiroplasma citri* strain GII3 was originally isolated from its leafhopper vector *Circulifer haematoceps* captured in Morocco (49). The low-passage, wild-type strain GII3 contains seven plasmids, pSciA and pSci1 to pSci6 (31). The *S. citri* GII3 mutant G/6 was engineered through plasmid incompatibility curing and only contains the pSciA and pSci6 plasmids; therefore, it lacks ScARP genes (29). Spiroplasmas that expressed the FD92-P VmpA at their cell surface were obtained by electro-transformation of the *S. citri* GII3 mutant G/6 with 1-5 µg of purified plasmid pSTVA1, as described by Renaudin and colleagues in (19). In summary, this plasmid carries the signal peptide depleted-*vmpA* coding sequence fused to the signal peptide sequence of the adhesin ScARP3d and is under the control of the *S. citri tuf* gene promoter and ribosome binding site (RBS). Spiroplasmas were cultivated at 32°C in SP4 medium from which the fresh yeast extract was omitted (50), and the medium

was supplemented with 5-10 µg/mL tetracycline when necessary. Colonies were further propagated in broth medium SP4 containing 5-10 µg/mL tetracycline during 3 passages and submitted to a dot blot immunoassay and Western blotting (see below) to reveal the production of VmpA.

Establishment of the Euva-1 cell line derived from the leafhopper *E. variegatus*

The cell line Euva-1 of the leafhopper *E. variegatus* was established according to a previously described protocol (27). Primary cell cultures, originally established from eggs with red eyespots, were maintained in monolayer culture at 25°C in culture medium made of 400 mL Schneider's *Drosophila* medium, 50 mL Grace's insect cell culture medium (Invitrogen), 50 mL heat-inactivated fetal bovine serum (Eurobio), 3 mL G-5 supplement (Invitrogen) supplemented with 1.25 µg.mL⁻¹ fungizone (Invitrogen) and 50 µgmL⁻¹ penicillin/streptomycin (Invitrogen). After the cell line was established, leafhopper cells were passed every 10 days with a 2/3 dilution with an additional change of the medium during the week.

DNA isolation, restriction and PCR

To confirm the origin of the cells, the genomic DNA was extracted from 20 mL culture of Euva-1 cells with the Wizard Genomic DNA purification kit (Promega). A fragment of approximately 800 bp of the cytochrome oxidase subunits I and II (COI) mitochondrial gene was amplified using the primers C1-J-2195 (5'-TTGATTTTTTGGTCATCCAGAAGT-3') and TL2-N-3014 (5'-TCCAATGCACTAATCTGCCATATTA-3') (51). PCR amplifications were performed according to Bertin *et al.* (52) with 1 µL of DNA template in a final volume of 25 µL. The sequencing of the PCR products from both the 5' and 3' end of purified PCR products was

performed by Beckman Coulters Genomics (Takeley, United Kingdom). The sequences were deposited in ENA (accession numbers LT960658 and LT960628).

Plasmid DNA was purified from 10 mL cultures of *Spiroplasma citri* with the Wizard SV Minipreps DNA Purification Kit (Promega). The plasmids were digested with *HindIII*, and the digested products were analyzed on 0.8% agarose gels. The amplification of the *vmpA* fragment was performed using the primers pSciF11 (5'-GTTATTGTGTGGGTCAGATG-3') and VmpARev (5'-CCCTAGCTAACTGAATTCATGGATC-3'). The PCR conditions were 35 cycles of 30 s at 92°C, 30 s at 52°C, and 45 s at 68°C with the Taq polymerase (Biolab).

Expression, purification of recombinant protein Vmps and production of antibodies

The primers Cl-VmpA-F1 (5'-ACAAACATATGAAAGCTATTACAGATTTGAGTGG-3'), Cl-VmpA-R1 (5'-TCATTCTCGAGTTAACTTTTTTCTTAACAGTAAAC-3'), Cl-VmpB-92F (5'-ATCAACATATGGCAGATAAAGAAAAACCATTATC-3') and Cl-VmpB-92R (5'-TAATTCTCGAGTTAGATTCTGTAACGGTTTCG-3') were designed for the cloning of a part of the *vmpA* (accession number LN680870) and *vmpB* genes (accession number PRJEB22700), respectively, without the trans-membrane regions, as detailed in figure S2A and S2B. The DNA fragments, 930 bp-long for VmpA (amino acids 38 to 347) and 756 bp-long for VmpB (aa 34 to 285), were PCR amplified with the Phusion High-Fidelity DNA polymerase (Finnzyme) from the total DNA of *V. faba* infected by FD92-P. For the expression of the histidine-tagged proteins in *Escherichia coli*, the amplicons were cloned into the pET28 expression system (Novagen, Madison, WI). *E. coli* BL21 Star (DE3) cells (Invitrogen) were then transformed with pet28-His₆-VmpA, pet-VmpA-His₆ or with pet28-His₆-VmpB, according to the manufacturer's protocol. Expression was induced with 1 mM IPTG. The tagged proteins were purified as described previously (24) on HIS-Select Nickel

affinity gel-packed columns (Sigma). For VmpA, the nickel column was conditioned with 0.05 M sodium phosphate buffer at pH 7.4 with 0.2% Triton X-100 and for VmpB with 0.05 M sodium phosphate buffer at pH 7.4 with 0.025 M imidazole and 0.2% Triton X-100. Imidazole elution concentrations were respectively 0.25 M for His₆-VmpA and 0.5 M for His-VmpB. The purification of each protein was monitored by sodium dodecyl sulfate-polyacrylamide gel electrophoresis (SDS PAGE), and Western blotting was applied with anti-FD monoclonal antibodies provided by the Sediag Company for His₆-VmpA/VmpA-His₆ and with the anti-Histidine antibodies (Sigma) for His₆-VmpB. Rabbit polyclonal antibodies (PABs) raised against the His₆-tagged recombinant VmpA (His₆-VmpA) (19) and the His₆-tagged recombinant VmpB (His₆-VmpB) were produced by Covalab (Villeurbanne, France).

Western immunoblotting and dot blot immunoassay

Immunoblotting analysis of spiroplasmal proteins has been previously described (53). Briefly, spiroplasmas were pelleted from 20 mL cultures by centrifugation at 25,000 g for 20 min and washed twice in HEPES-sucrose (HS) buffer (8 mM HEPES [pH 7.4] and 280 mM sucrose). Protein concentrations were determined using the DC Protein Assay Kit (Bio-Rad, Hercules, CA, USA). Protein preparations were mixed with one volume of 2× Laemmli solubilization buffer and solubilized by heating at 80°C for 20 min. The preparation was stored at -20°C until use or directly separated by 10% SDS-PAGE, and then, the proteins were electro-transferred to a nitrocellulose membrane. For dot blotting, spiroplasmas from 2 mL culture were spotted onto nitrocellulose membrane after two washes in HEPES-sucrose (HS) buffer. The presence of VmpA was revealed using anti-His₆-VmpA PABs (1:5000 dilution), goat anti-rabbit immunoglobulin G-alkaline phosphatase conjugate and NBT-BCIP (Sigmafast™, Sigma-Aldrich, St Louis, MO, USA) as the substrate.

Coating of fluorescent beads

The yellow-green fluorescent and amine-modified beads (4×10^9 beads at $1 \mu\text{m}$) (Invitrogen) were covalently coated with 10 nmol of a mix of recombinant VmpA-His₆ and GFP or BSA, according to the supplier's instructions. The relative quantity of VmpA-His₆, GFP and BSA varied according the experiments and are indicated under the graphs. The coating of the beads was verified by immunofluorescence. VmpA-His₆-coated beads were incubated with anti-VmpA PABs diluted 1:500 in PBS-BSA solution (PBS containing 1% BSA) for 30 min; after 3 washes with PBS, the beads were incubated for 30 min with Alexa 633-conjugated goat anti-rabbit antibodies (Invitrogen) diluted at 1:200. The beads were included in the anti-fading ProLong Gold Reagent (Invitrogen), mounted with cover slips and imaged using a TCS SP2 upright Leica confocal laser scanning microscope (CLSM), with a 63x oil immersion objective lens with a pixel size of 70 nm. Fluorochromes were detected sequentially frame by frame. The coating of fluorescent beads was also verified for VmpA and BSA by measuring the remaining uncoated proteins using the Bradford procedure.

Coloration and microscopy of Euva-1 cells, salivary glands and midguts of *Euscelidius variegatus*

Euva-1 cells were grown on coverslips in 24-well plates for one day and then washed in PBS. The cells were fixed with 4% paraformaldehyde and incubated with methylene blue (0.1%) for one minute after 3 washes in water or with Alexa 568-Phalloidin (Thermo Fisher Scientific) and DAPI (SIGMA). Samples were mounted with ProLong Gold antifade reagent (Thermo Fisher Scientific) and imaged using a Nikon Eclipse E800 microscope with 40x and 20x objective lenses.

To infect *E. variegatus* with FD-P, 5th instar nymphs were fed phytoplasma-infected broad bean for one week, corresponding to the acquisition period. The insects were

subsequently caged on healthy broad bean for different latency periods in a greenhouse. The intestine and salivary glands were dissected from 10 insects. The organs were fixed with paraformaldehyde 4%, washed in PBS, incubated with a 1:3000 dilution of anti-VmpA rabbit serum (PABs) in PBS-BSA, washed and then incubated with Alexa 488-conjugated goat anti-rabbit IgG (Thermo Fisher Scientific) at a 1:200 dilution. F-actin and nuclei were stained using Alexa 568-Phalloidin (Thermo Fisher Scientific) and DAPI (SIGMA), respectively. Immunofluorescent samples were finally mounted with ProLong Gold antifade reagent (Thermo Fisher Scientific) and imaged using a TCS SP2 upright Leica confocal laser scanning microscope (CLSM) with X40 water immersion and X20 objective lens.

For transmission electron microscopy (TEM), the insects were fed in microtubes as described above with caps filled with HEPES-sucrose with or without VmpA-His₆-coated beads (6.6 nmol of recombinant VmpA-His₆ with 3.3 nmol of BSA) for two days and caged on healthy plants for one day. The dissected midguts were fixed in glutaraldehyde, post-fixed in osmium tetroxide, and dehydrated in ethanol, and inclusion was performed in Epon resin as described previously (24, 27). Micrographs were taken at 120 kV on an FEI Tecnai G2 Spirit equipped with an Eagle 4K digital camera (FEI France, Lyon).

Euva-1 adhesion assays

Adhesion assays of yellow-green fluorescent and amine-modified beads were performed as previously described (41). Briefly, Euva-1 cells cultivated on coverslips in 24-well plates were incubated with 2×10^6 coated latex beads in Schneider's *Drosophila* medium for 1 h at 25°C. After three washes, the cells were fixed with 4% paraformaldehyde, and the cell nuclei were stained with $1 \mu\text{gml}^{-1}$ DAPI for 5 min. The samples were mounted in the anti-fading ProLong Gold Reagent (Thermo Fisher Scientific), and immunofluorescent samples were analyzed with a fluorescence microscope (Nikon Eclipse E800) at 40×

magnification. Each experiment was repeated three times independently in triplicate. For each experiment, 20 to 25 fields with approximately 30 cells per field were observed randomly. Counting of beads per cell was performed with the free software package ImageJ (<http://imagej.nih.gov/ij/>). For the relative number of adherent beads per cells, the average of the bead number in the control condition (0 in figures 4 B and C) corresponded to a value of 1. The relative values of bead numbers obtained in the different conditions were then readjusted according to this endogenous standard. For the antibody inhibition assay, VmpA-His₆-coated beads were pre-incubated in the presence of various concentrations of anti-His₆-VmpA PABs (1/10 to 1/1 000) or anti-spiralin (54) for 1 h at room temperature. For the competitive assay, Euva-1 cells were pre-incubated for 1 h at 25°C in the presence of various quantities of His₆-VmpA (0.2 to 0.8 nmol) or His₆-VmpB (0.8 nmol). After one wash in PBS, the fluorescent VmpA-His₆-coated beads were added to the Euva-1 cells as above. Each experiment was repeated three times independently in triplicate.

The binding of spiroplasmas that express VmpA to Euva-1 cells were determined essentially as described previously in (27). In brief, approximately 10⁵ Euva-1 cells per well were infected with *S. citri* at a multiplicity of infection between 20 and 50 and incubated at 30°C for 3 h. The insect cells were trypsinized with TrypLE (Thermo Fisher Scientific) for 5 min. Serial dilutions were plated onto SP4 containing 1% noble agar for colony forming units (cfu) counting. To calculate the relative percentage of adherent spiroplasmas, the value 100% corresponded to the average of the adherent *S. citri* G/6/pSTP2 (control condition). Each experiment was performed in four distinct wells and was repeated three times.

Ingestion assays

HEPES-sucrose solution (500 µL) containing 10⁵ coated beads was introduced in the cap of 1.5 mL microtubes and closed with parafilm. Three young adults of *E. variegatus* were

introduced by tube containing a narrow band of Whatman paper to allow the insects to move up to the cap, and a piece of gauze placed just below the cap to permit the insect to hold on to it and eat. After 2 days at room temperature, to ensure insect adaptation to the artificial feeding system, the 25 to 30 surviving insects (approximately 80%) were transferred into a cage containing 2 broad beans. One, four and seven days later, 20 insects were dissected. Other experiments with insects left two days on broad beans were independently conducted beside the first set of experiments but were shown on the same graph in figure 6. The midguts were fixed for 18 h with 4% paraformaldehyde in PBS containing 0.1% Triton X-100. Alexa 568-phalloidin (Invitrogen) was used to stain the actin filaments (diluted 1:200 in PBS-BSA for 1 h) and DAPI (SIGMA) to stain nuclei (for 5 min in water). The organs were mounted in anti-fading ProLong Gold Reagent (Invitrogen), and immunofluorescent samples were imaged using the fluorescence microscope Nikon Eclipse E800. For each experiment, approximately 15 midguts were observed per condition, and the experimentation was repeated three times. Counting of beads per midgut and the determination of the area of midguts were performed with the free software package ImageJ (<http://imagej.nih.gov/ij/>).

Statistical analyses

The similarities of deviations between independent experiments were checked with the F-test first. Then, for the purposes of statistical evaluation, Student's t-test was used for comparing two samples, and Student's z-test was used for comparing four samples. The results of the statistical analyses using tests were considered to be significant if their corresponding P values were less than 0.05 (*) and 0.001 (**).

ACKNOWLEDGMENTS

We are grateful to L. Brocard of the Bordeaux Imaging Center and the subgroup of the France Bioimaging Infrastructure for advice and experimental assistance in the preparation of samples for transmission electron microscopy. The authors gratefully acknowledge K. Guionneau and D. Lacaze for rearing the insects and producing the plants. This research was funded by the Conseil Interprofessionnel du Vin de Bordeaux, FranceAgriMer, the Regional Council of Aquitaine region, and INRA in the frame of the project “VMP Adapt” of the Plant Health and Environment.

References

1. Lee I-M, Davis RE, Gundersen-Rindal DE. 2000. Phytoplasma: Phytopathogenic Mollicutes. *Annu Rev Microbiol* 54:221–255.
2. Sugio A, MacLean AM, Kingdom HN, Grieve VM, Manimekalai R, Hogenhout SA. 2011. Diverse Targets of Phytoplasma Effectors: From Plant Development to Defense Against Insects. *Annu Rev Phytopathol* 49:175–195.
3. Weintraub PG, Beanland L. 2006. Insect Vectors of Phytoplasmas. *Annu Rev Entomol* 51:91–111.
4. Hogenhout SA, Oshima K, Ammar E-D, Kakizawa S, Kingdom HN, Namba S. 2008. Phytoplasmas: bacteria that manipulate plants and insects. *Mol Plant Pathol* 9:403–423.
5. Schvester D, Carle P, Moutous G. 1961. Sur la transmission de la flavescence dorée des vignes par une cicadelle. *Comptes Rendus Académie Sci* 18:1021–1024.
6. EFSA Panel on Plant Health (PLH), Jeger M, Bragard C, Caffier D, Candresse T, Chatzivassiliou E, Dehnen-Schmutz K, Gilioli G, Jaques Miret JA, MacLeod A, Navajas

562 Navarro M, Niere B, Parnell S, Potting R, Rafoss T, Rossi V, Urek G, Van Bruggen A,
563 Van Der Werf W, West J, Winter S, Bosco D, Foissac X, Strauss G, Hollo G, Mosbach-
564 Schulz O, Grégoire J-C. 2016. Risk to plant health of Flavescence dorée for the EU
565 territory. EFSA J 14:n/a-n/a.

566 7. Boudon-Padieu E, Larrue J, Caudwell A. 1989. ELISA and dot-blot detection of
567 flavescence dorée-MLO in individual leafhopper vectors during latency and inoculative
568 state. Curr Microbiol 19:357–364.

569 8. Maillet PL, Gouranton J. 1971. Etude du cycle biologique du mycoplasme de la
570 phyllodie du trèfle dans l'insecte vecteur, *Euscelis lineolatus* Brulle (Homoptera,
571 Jassidae). J Microsc.

572 9. Gouranton J, Maillet P. 1973. High-Resolution Autoradiography of Mycoplasma-like
573 Organisms Multiplying. J Invertebr Pathol 21:158–163.

574 10. Lefol C, Lherminier J, Boudonpadieu E, Larrue J, Louis C, Caudwell A. 1994.
575 Propagation of Flavescence Doree Mlo (mycoplasma-Like Organism) in the Leafhopper
576 Vector *Euscelidius-Variegatus* Kbm. J Invertebr Pathol 63:285–293.

577 11. Bressan A, Girolami V, Boudon-Padieu E. 2005. Reduced fitness of the leafhopper
578 vector *Scaphoideus titanus* exposed to Flavescence doree phytoplasma. Entomol Exp
579 Appl 115:283–290.

580 12. Fletcher J, Wayadande A, Melcher U, Ye F. 1998. The phytopathogenic mollicute-insect
581 vector interface: A closer look RID E-7160-2010. Phytopathology 88:1351–1358.

582 13. Liu H-Y. 1983. The Relationship of *Spiroplasma citri* and *Circulifer tenellus*.
583 Phytopathology 73:585.

14. Kakizawa S, Oshima K, Nishigawa H, Jung H-Y, Wei W, Suzuki S, Tanaka M, Miyata S, Ugaki M, Namba S. 2004. Secretion of immunodominant membrane protein from onion yellows phytoplasma through the Sec protein-translocation system in *Escherichia coli*. *Microbiol Read Engl* 150:135–142.
15. Suzuki S, Oshima K, Kakizawa S, Arashida R, Jung H-Y, Yamaji Y, Nishigawa H, Ugaki M, Namba S. 2006. Interaction between the membrane protein of a pathogen and insect microfilament complex determines insect-vector specificity. *Proc Natl Acad Sci U S A* 103:4252–4257.
16. Galetto L, Bosco D, Balestrini R, Genre A, Fletcher J, Marzachì C. 2011. The major antigenic membrane protein of “*Candidatus Phytoplasma asteris*” selectively interacts with ATP synthase and actin of leafhopper vectors. *PloS One* 6:e22571.
17. Rashidi M, Galetto L, Bosco D, Bulgarelli A, Vallino M, Veratti F, Marzachì C. 2015. Role of the major antigenic membrane protein in phytoplasma transmission by two insect vector species. *BMC Microbiol* 15:193.
18. Cimerman A, Pacifico D, Salar P, Marzachì C, Foissac X. 2009. Striking Diversity of vmp1, a Variable Gene Encoding a Putative Membrane Protein of the Stolbur Phytoplasma. *Appl Environ Microbiol* 75:2951–2957.
19. Renaudin J, Béven L, Batailler B, Duret S, Desqué D, Arricau-Bouvery N, Malembic-Maher S, Foissac X. 2015. Heterologous expression and processing of the flavescence dorée phytoplasma variable membrane protein VmpA in *Spiroplasma citri*. *BMC Microbiol* 15:82.

- 605 20. Carle P, Malembic-Maher S, Arricau-Bouvery N, Desqué D, Eveillard S, Carrere S,
606 Foissac X. 2011. Flavescence doree' phytoplasma genome: a metabolism oriented
607 towards glycolysis and protein degradation. *Bull Insectology* 64:S13–S14.
- 608 21. Dramsi S, Dehoux P, Cossart P. 1993. Common features of Gram-positive bacterial
609 proteins involved in cell recognition. *Mol Microbiol* 9:1119–1122.
- 610 22. Yu J, Wayadande AC, Fletcher J. 2000. *Spiroplasma citri* Surface Protein P89
611 Implicated in Adhesion to Cells of the Vector *Circulifer tenellus*. *Phytopathology*
612 90:716–722.
- 613 23. Berg M, Melcher U, Fletcher J. 2001. Characterization of *Spiroplasma citri* adhesion
614 related protein SARP1, which contains a domain of a novel family designated sarpin.
615 *Gene* 275:57–64.
- 616 24. Béven L, Duret S, Batailler B, Dubrana M-P, Saillard C, Renaudin J, Arricau-Bouvery
617 N. 2012. The repetitive domain of ScARP3d triggers entry of *Spiroplasma citri* into
618 cultured cells of the vector *Circulifer haematocephus*. *PLoS ONE* 7:e48606.
- 619 25. Glew MD, Papazisi L, Poumarat F, Bergonier D, Rosengarten R, Citti C. 2000.
620 Characterization of a multigene family undergoing high-frequency DNA rearrangements
621 and coding for abundant variable surface proteins in *Mycoplasma agalactiae*. *Infect*
622 *Immun* 68:4539–4548.
- 623 26. Fleury B, Bergonier D, Berthelot X, Peterhans E, Frey J, Vilei EM. 2002.
624 Characterization of P40, a Cytadhesin of *Mycoplasma agalactiae*. *Infect Immun*
625 70:5612–5621.

- 626 27. Duret S, Batailler B, Danet J-L, Béven L, Renaudin J, Arricau-Bouvery N. 2010.
627 Infection of the *Circulifer haematoceps* cell line Ciha-1 by *Spiroplasma citri*: the non-
628 insect-transmissible strain 44 is impaired in invasion. *Microbiol Read Engl* 156:1097–
629 1107.
- 630 28. Caudwell A, Larrue J. 1977. La production de cicadelles saines et infectieuses pour les
631 épreuves d'infectivité chez les jaunisses à mollicutes des végétaux. L'élevage de
632 *Euscelidius variegatus* KBM et la ponte sur mousse de polyurethane. *Ann Zool Ecol*
633 *Anim* 9:443–456.
- 634 29. Breton M, Duret S, Danet J-L, Dubrana M-P, Renaudin J. 2010. Sequences essential for
635 transmission of *Spiroplasma citri* by its leafhopper vector, *Circulifer haematoceps*,
636 revealed by plasmid curing and replacement based on incompatibility. *Appl Environ*
637 *Microbiol* 76:3198–3205.
- 638 30. Breton M, Duret S, Arricau-Bouvery N, Béven L, Renaudin J. 2008. Characterizing the
639 replication and stability regions of *Spiroplasma citri* plasmids identifies a novel
640 replication protein and expands the genetic toolbox for plant-pathogenic spiroplasmas.
641 *Microbiol Read Engl* 154:3232–3244.
- 642 31. Saillard C, Carle P, Duret-Nurbel S, Henri R, Killiny N, Carrère S, Gouzy J, Bové J-M,
643 Renaudin J, Foissac X. 2008. The abundant extrachromosomal DNA content of the
644 *Spiroplasma citri* GII3-3X genome. *BMC Genomics* 9:195.
- 645 32. Aiba S, Tsunekawa H, Imanaka T. 1982. New approach to tryptophan production by
646 *Escherichia coli*: genetic manipulation of composite plasmids *in vitro*. *Appl Environ*
647 *Microbiol* 43:289–297.

- 648 33. Rai M, Padh H. 2001. Expression systems for production of heterologous proteins. *Curr*
649 *Sci* 80:1121–1128.
- 650 34. Steen A, Wiederhold E, Gandhi T, Breitling R, Slotboom DJ. 2011. Physiological
651 adaptation of the bacterium *Lactococcus lactis* in response to the production of human
652 CFTR. *Mol Cell Proteomics MCP* 10:M000052MCP200.
- 653 35. Hattab G, Suisse AYT, Illoaia O, Casiraghi M, Dezi M, Warnet XL, Warschawski DE,
654 Moncoq K, Zoonens M, Miroux B. 2014. Membrane Protein Production in *Escherichia*
655 *coli*: Overview and Protocols, p. 87–106. *In* *Membrane Proteins Production for*
656 *Structural Analysis*. Springer, New York, NY.
- 657 36. Cheung WWK, Purcell AH. 1993. Ultrastructure of the digestive system of the Le
658 fopper *Euscelidius variegatus* Kirshbaum (Homoptera : Cicadellidae), with and without
659 congenital bacterial infections. *Int J Insect Morphol Embryol* 22:49–61.
- 660 37. García González J, Ossamu Tanaka FA, Spotti Lopes JR. 2015. First Findings in the
661 Route of the Maize Bushy Stunt Phytoplasma Within Its Vector *Dalbulus maidis*
662 (Hemiptera: Cicadellidae). *J Econ Entomol*.
- 663 38. Silva CP, Silva JR, Vasconcelos FF, Petretski MDA, Damatta RA, Ribeiro AF, Terra
664 WR. 2004. Occurrence of midgut perimicrovillar membranes in paraneopteran insect
665 orders with comments on their function and evolutionary significance. *Arthropod Struct*
666 *Dev* 33:139–148.
- 667 39. Gutiérrez-Cabrera AE, Córdoba-Aguilar A, Zenteno E, Lowenberger C, Espinoza B.
668 2016. Origin, evolution and function of the hemipteran perimicrovillar membrane with
669 emphasis on Reduviidae that transmit Chagas disease. *Bull Entomol Res* 106:279–291.

- 670 40. Alves CR, Albuquerque-Cunha JM, Mello CB, Garcia ES, Nogueira NF, Bourguignon
671 SC, de Souza W, Azambuja P, Gonzalez MS. 2007. Trypanosoma cruzi: Attachment to
672 perimicrovillar membrane glycoproteins of Rhodnius prolixus. Exp Parasitol 116:44–52.
- 673 41. Duret S, Batailler B, Dubrana M-P, Saillard C, Renaudin J, Béven L, Arricau-Bouvery
674 N. 2014. Invasion of insect cells by Spiroplasma citri involves spiralin relocalization and
675 lectin/glycoconjugate-type interactions. Cell Microbiol 16:1119–1132.
- 676 42. Killiny N, Castroviejo M, Saillard C. 2005. Spiroplasma citri Spiralin Acts In Vitro as a
677 Lectin Binding to Glycoproteins from Its Insect Vector Circulifer haematiceps.
678 Phytopathology 95:541–548.
- 679 43. Peng J, Zhong J, R. Granados R. 1999. A baculovirus enhancer alters the permeability of
680 a mucosal midgut peritrophic matrix from lepidopteran larvae. J Insect Physiol 45:159–
681 166.
- 682 44. Yeats C, Rawlings ND, Bateman A. 2004. The PepSY domain: a regulator of peptidase
683 activity in the microbial environment? Trends Biochem Sci 29:169–172.
- 684 45. Killiny N, Batailler B, Foissac X, Saillard C. 2006. Identification of a Spiroplasma citri
685 hydrophilic protein associated with insect transmissibility. Microbiol Read Engl
686 152:1221–1230.
- 687 46. Caudwell A, Kuszala C, Bachelier JC, Larrue J. 1970. Transmission de la Flavescence
688 dorée de la vigne aux plantes herbacées par l’allongement du temps d’utilisation de la
689 cicadelle Scaphoideus littoralis Ball et l’étude de sa survie sur un grand nombre
690 d’espèces végétales. Ann Phytopathol 1572(Hors série):181–9.

- 691 47. Angelini E, Clair D, Borgo M, Bertaccini A, Boudon-Padieu E. 2001. Flavescence doree
692 in France and Italy - Occurrence of closely related phytoplasma isolates and their near
693 relationships to Palatinate grapevine yellows and an alder yellows phytoplasma. VITIS -
694 J Grapevine Res 40:79–86.
- 695 48. Caudwell A, Kuszla C, Larrue J, Bachelier JC. 1972. Transmission de la flavescence
696 doree de la feve a la feve par des cicadelles des genres Euscelis et Euscedlidius:
697 Intervention possible de ces insectes dans l'epidemiologie du bois noir en Bourgogne.
698 Ann Phytopathol.
- 699 49. Vignault JC, Bové JM, Saillard C, Vogel R, Faro A, Venegas L, Stemmer W, Aoki S,
700 McCoy R, Al-Beldawi A, Larue M, Tuzcu O, Ozsan M, Nhami A, Abassi M, Bonfils J,
701 Moutous G, Fos A, Poutiers F, Viennot-Bourgin G. 1980. Mise en culture de
702 spiroplasmes à partir de matériel végétal et d'insectes provenant de pays circum
703 méditerranéens et du Proche Orient. C R Acad Sci Ser III 290:775–780.
- 704 50. Tully JG, Whitcomb RF, Clark HF, Williamson DL. 1977. Pathogenic mycoplasmas:
705 cultivation and vertebrate pathogenicity of a new spiroplasma. Science 195:892–894.
- 706 51. Simon C, Frati F, Beckenbach A, Crespi B, Liu H, Flook P. 1994. Evolution, Weighting,
707 and Phylogenetic Utility of Mitochondrial Gene-Sequences and a Compilation of
708 Conserved Polymerase Chain-Reaction Primers. Ann Entomol Soc Am 87:651–701.
- 709 52. Bertin S, Picciau L, Ács Z, Alma A, Bosco D. 2010. Molecular identification of the
710 Hyalesthes species (Hemiptera: Cixiidae) occurring in vineyard agroecosystems. Ann
711 Appl Biol 157:435–445.
- 712 53. Duret S, Berho N, Danet J-L, Garnier M, Renaudin J. 2003. Spiraline is not essential for
713 helicity, motility, or pathogenicity but is required for efficient transmission of

Spiroplasma citri by its leafhopper vector Circulifer haematocephus. Appl Environ
Microbiol 69:6225–6234.

54. Wróblewski H, Johansson KE, Hjérten S. 1977. Purification and characterization of
spiralin, the main protein of the Spiroplasma citri membrane. Biochim Biophys Acta
465:275–289.

FIGURE LEGEND

Figure 1. Confocal micrographs of *Euscelidius variegatus*-infected leafhoppers' midgut immunolabeled with anti-VmpA PABs. The midguts of leafhoppers that were fed healthy broad bean or FD-P infected broad bean were observed with fluorescent and differential interference contrast (DIC) microscopy. Actin was labeled with Alexa 568-phalloidin (red), nuclei was labeled with DAPI (blue), and FD-P was labeled with anti-His₆-VmpA PABs and secondary Alexa 488-antibodies (green). Arrows indicate internal phytoplasmas, and arrowheads show the phytoplasmas that were located close to actin filaments.

Figure 2. Confocal micrographs of *E. variegatus*-infected leafhoppers' salivary glands immunolabeled with anti-VmpA PABs. The salivary gland cells of leafhopper fed healthy broad bean or FD-P infected broad bean were observed with fluorescent and differential interference contrast (DIC) microscopy. Actin was labeled with Alexa 568-phalloidin (red), nuclei were stained with DAPI (blue), and FD-P was labeled with anti-His₆-VmpA PABs and secondary Alexa 488-antibodies (green).

Figure 3. Observation of Euva-1 cells cultured from *E. variegatus* embryos by phase contrast (A) and epifluorescence (B) microscopy. (A) Low magnification (x20, a) and high magnification (x40, b) of the Euva-1 monolayer colored with methylene blue. Cells that have

their nucleus colored by methylene blue are indicated by red asterisks. Cells with both the nucleus and cytosol colored by methylene blue are indicated by arrows for the larger ones or arrowheads for the smaller ones. (B) Cellular actin was labeled with Alexa 568-phalloidin (green), and nuclei were stained with DAPI (blue). (A) and (B) same magnification; scale bar, 50 μ m (a) and 20 μ m (b).

Figure 4. Adhesion of VmpA-His₆-coated fluorescent beads to Euva-1 cells. (A) Observation of fluorescent VmpA-coated beads adherent to Euva-1 cells. (a) Fluorescent VmpA-coated beads (green), (b) nuclei were stained with DAPI (light blue), (c) overlay, and (d) same view by differential interference contrast microscopy. Scale bar 20 μ m. (B). Fluorescent beads were coated with different amounts of VmpA-His₆ and GFP before coming in contact with insect cells in culture. ** and * indicates significant differences compared to beads coated with 0 nmol of VmpA-His₆ and 10 nmol of GFP (Student's test, P<0.01 and P<0.05, respectively). (C) The fluorescent beads coated with VmpA-His₆ were pre-incubated with rabbit serum anti-His₆-VmpA (gray bars) or anti-spiralin (control, white bars) at the indicated dilutions. * indicates a significant difference compared to non-treated beads (0) (Student's test, P<0.05). (D) Euva-1 cells were pre-incubated with the recombinant protein His₆-VmpA (gray bar) or His₆-VmpB (white bar) at the indicated concentrations. *, significantly different from Euva-1 pre-incubated with medium alone (0) (Student's test, P<0.05).

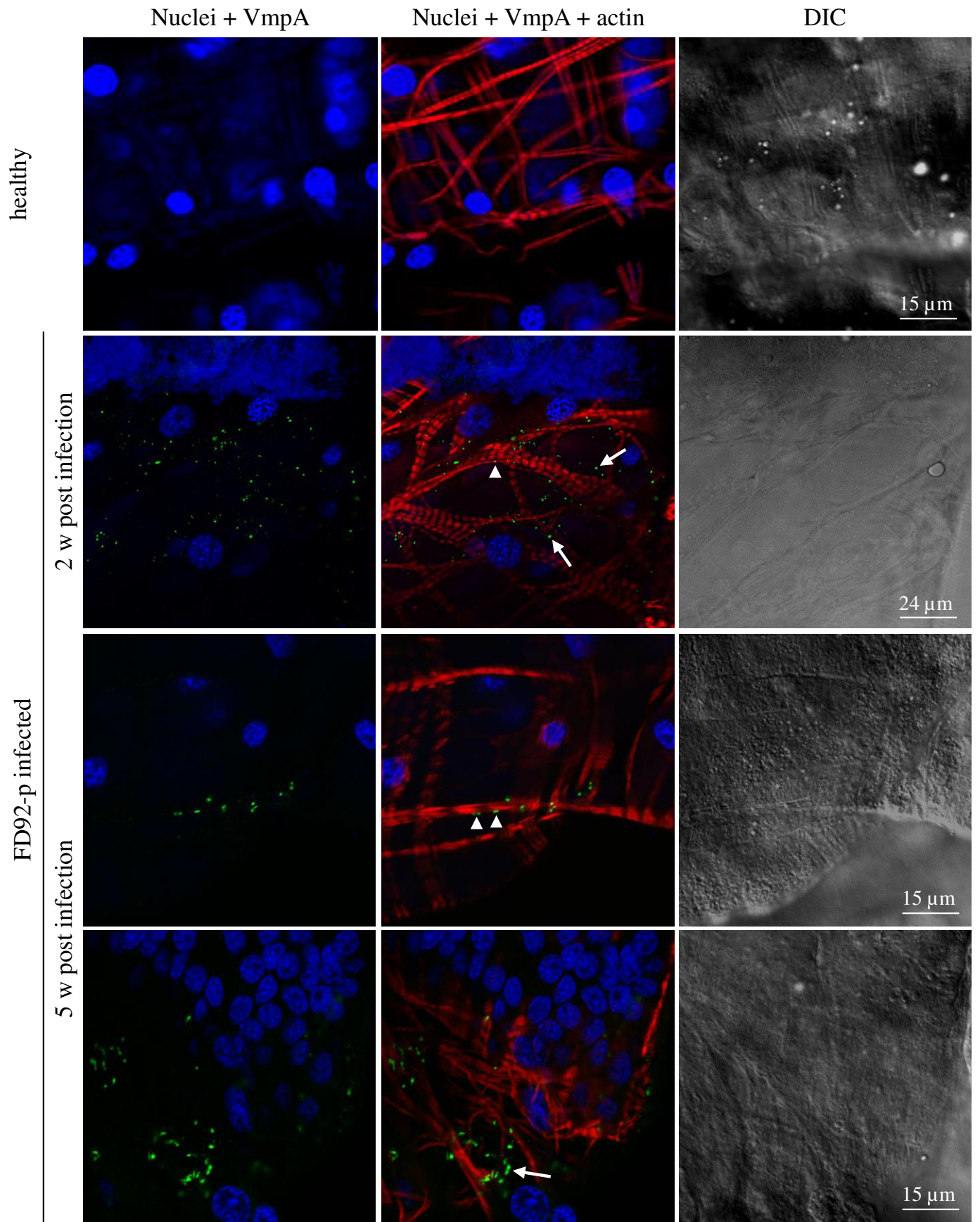
Figure 5. Expression of VmpA by *Spiroplasma citri* and the adhesion of VmpA-expressing *S. citri* to Euva-1 cells. (A) Plasmid extractions and restriction with *Hind*III enzyme (plasmid profile), PCR amplification of the *vmpA* gene and Western immunoblotting of proteins from *S. citri* transformants. Sub-clones of the two clones 5 and 6 of VmpA

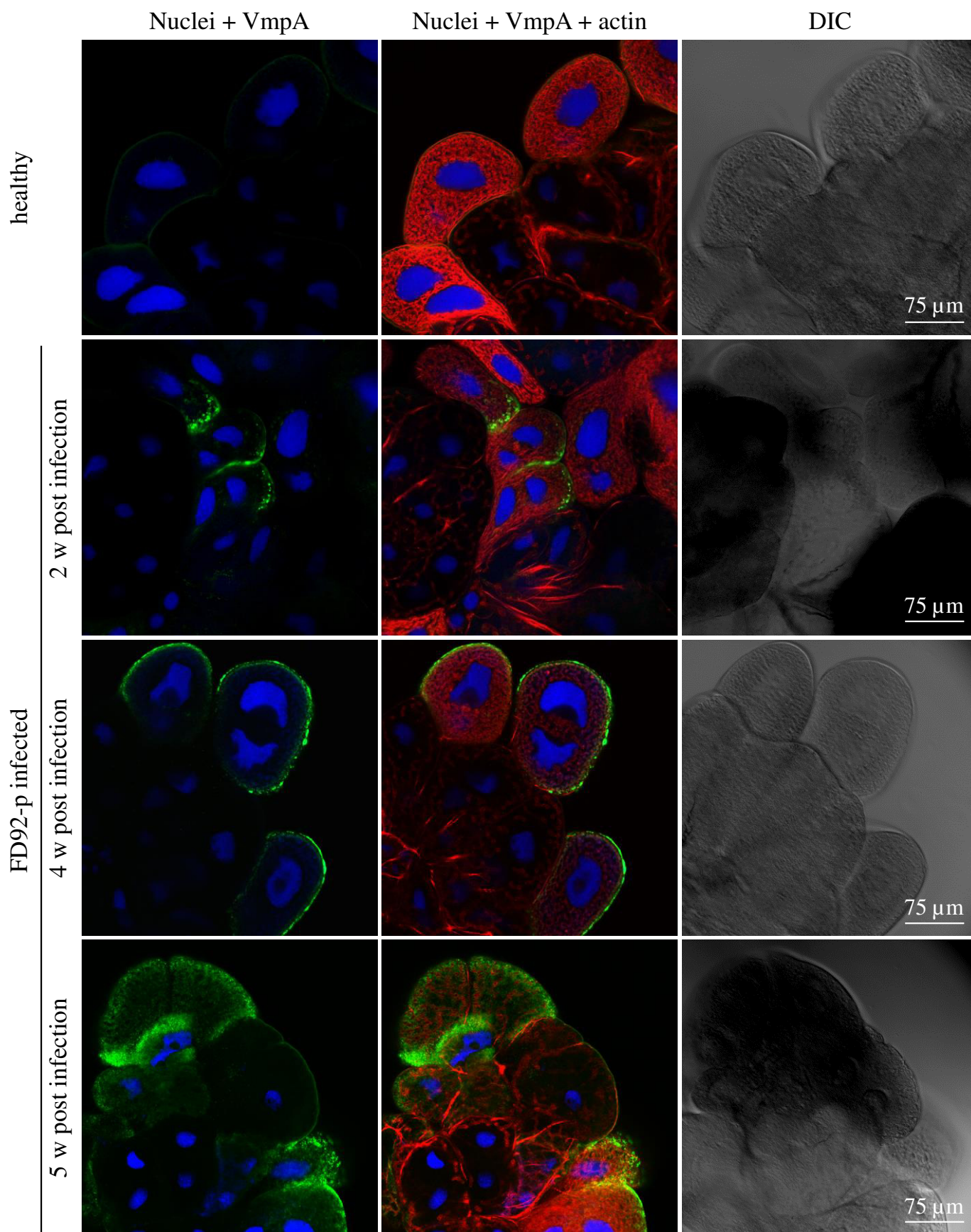
expressing *S. citri* were cultivated without tetracycline (-) or in the presence of tetracycline (+) for 5 passages prior to extractions. The blot was probed with a 1:5000 dilution of anti-His₆-VmpA rabbit serum. Lane 1 kb +: 1 kb Plus DNA ladder; lane +: plasmid pSTVA1; lane MW: molecular weight in kDa; lane rVmpA: recombinant protein VmpA lacking the C-terminal transmembrane segment. (B) The Adhesion of *S. citri* transformants to Euva-1 cells. The 100% relative corresponds to the condition of cell adhesion with *S. citri* G/6 strain carrying the plasmid pSTP2. **, significantly different from Euva-1 infected with *S. citri* G/6/pSTP2 devoid of VmpA (Student's test, P<0.001).

Figure 6. Number of VmpA-His₆-coated latex beads in *E. variegatus* midguts after ingestion and fluorescent observations. (A) The presence of fluorescent beads coated with VmpA-His₆ in *E. variegatus* midgut after the ingestion of beads for two days. Low magnification (x4) by fluorescence microscopy (a) showing the actin fluorescence (red, Alexa 568-phalloidin) of intestine cells and fluorescent beads (green) and by phase-contrast microscopy overlaid with fluorescent image of beads (b). amg, anterior midgut; mmg, middle midgut; pmg, posterior midgut; fc, filter chamber; mt, Malpighian tubules. (c, d and e) Higher magnification showing VmpA-His₆-coated latex beads (green) (c), actin (red) and nuclei (blue, DAPI) (d), and the overlay of green VmpA-His₆-coated latex beads and intestine tube viewed by phase-contrast microscopy (e). (B) The number of VmpA-His₆-coated beads in the *E. variegatus* middle midgut. After feeding HEPES-sucrose with BSA-coated beads (white circles) or with VmpA-His₆-coated beads (black and gray circles), *E. variegatus* insects were maintained one, two, four or seven days on broad bean before their intestines were dissected. These assays were performed in three independent experiments, and 36 to 70 insects per group were examined. Different lowercase letters above sets indicate statistically significant differences calculated separately for each time on broad bean (Student's test, P<0.05).

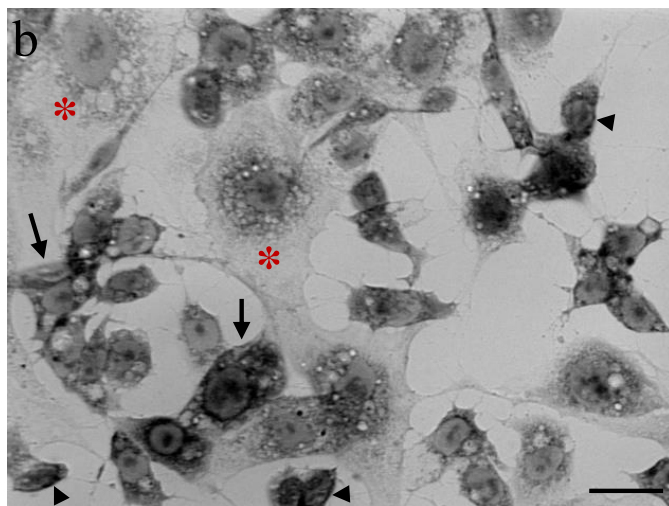
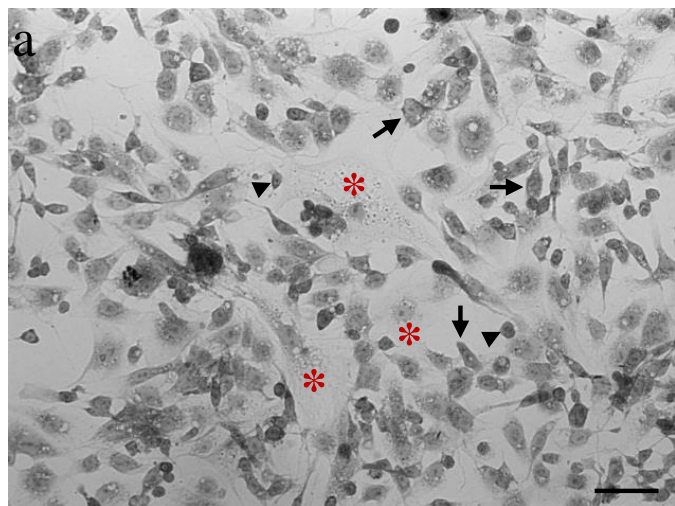
789

790 **Figure 7. Transmission electron microscopy images of the dissected midgut of *E.***
791 ***variegatus* that have ingested VmpA-H₆-coated fluorescent beads.** (A) The anterior (a) and
792 middle (b and c) midgut of one healthy insect. (c) shows the high magnification of the boxed
793 part of (b). (B and C) A section of the anterior (B) and middle (C) midgut of an insect that
794 was fed VmpA-His6-coated beads in HEPES-sucrose for two days. (B b) and (B c) show
795 different magnifications of the boxed part of (B a). (C b) and (C c) represent higher
796 magnifications of the boxed parts of (C a). Beads are shown with asterisks and bacteria with
797 arrowheads. L, lumen; mv, microvillosity; pmm, perimicrovillar membrane.

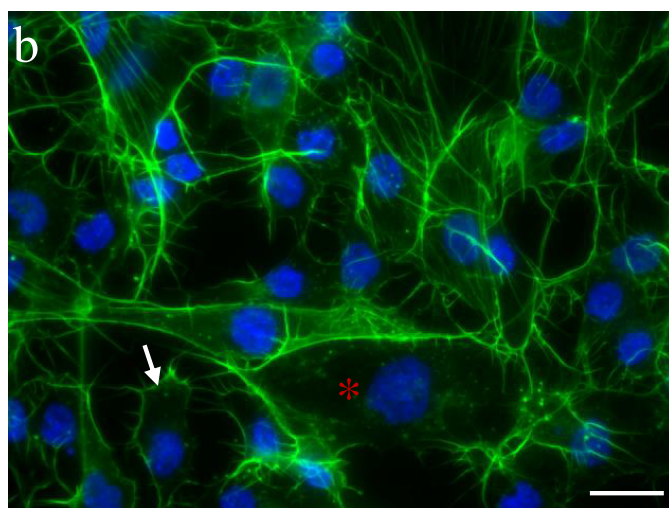
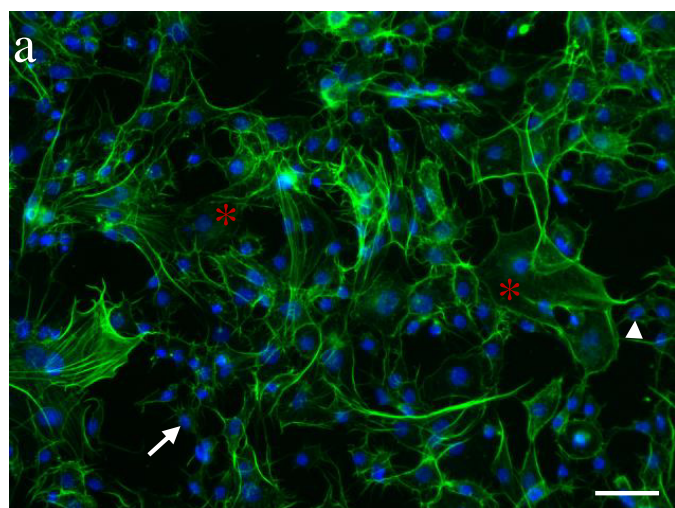


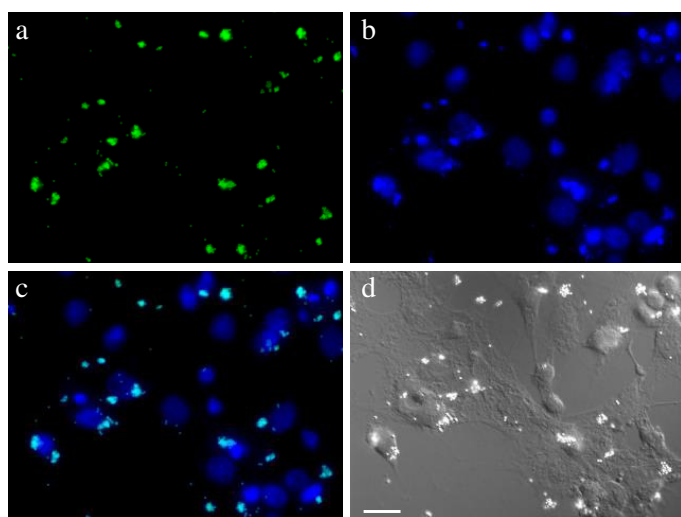
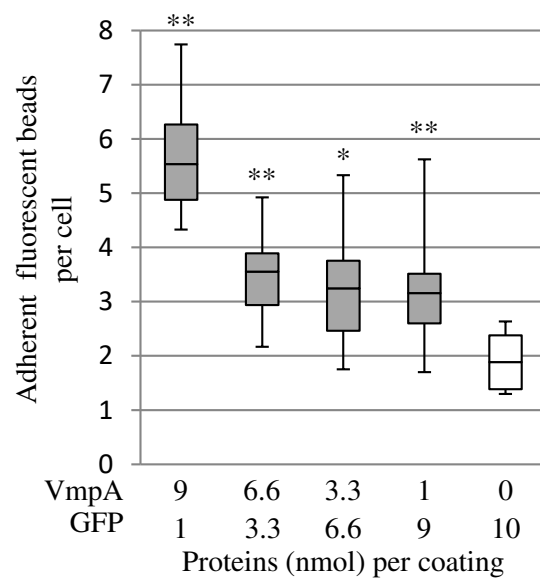
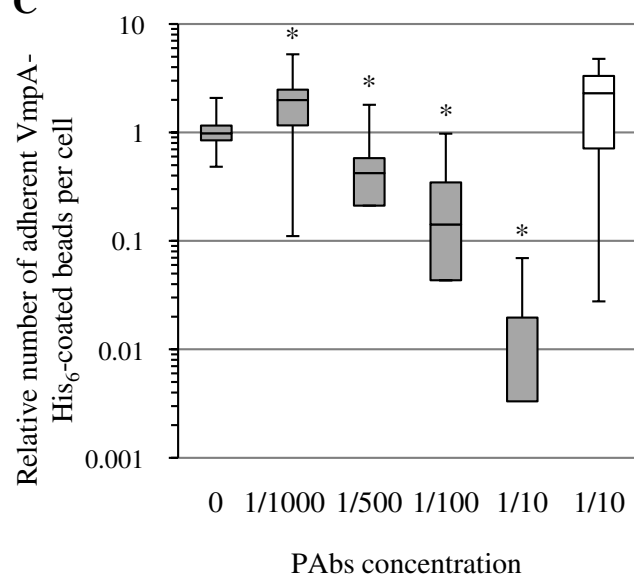
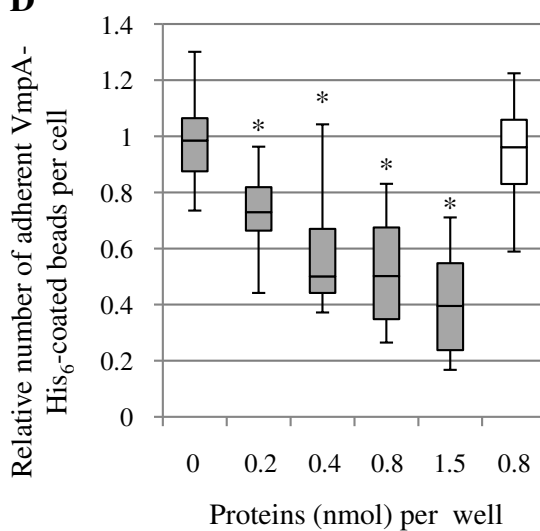


A

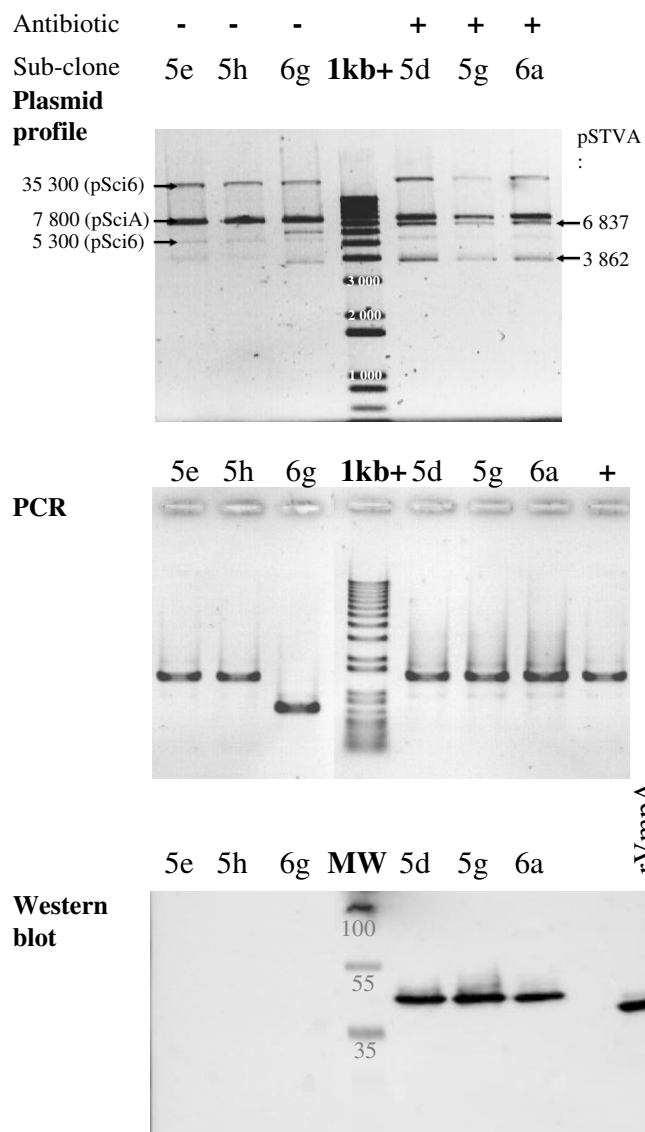


B

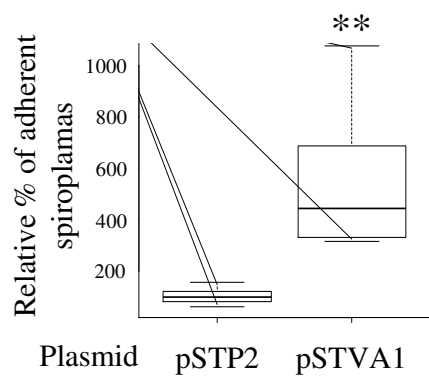


A**B****C****D**

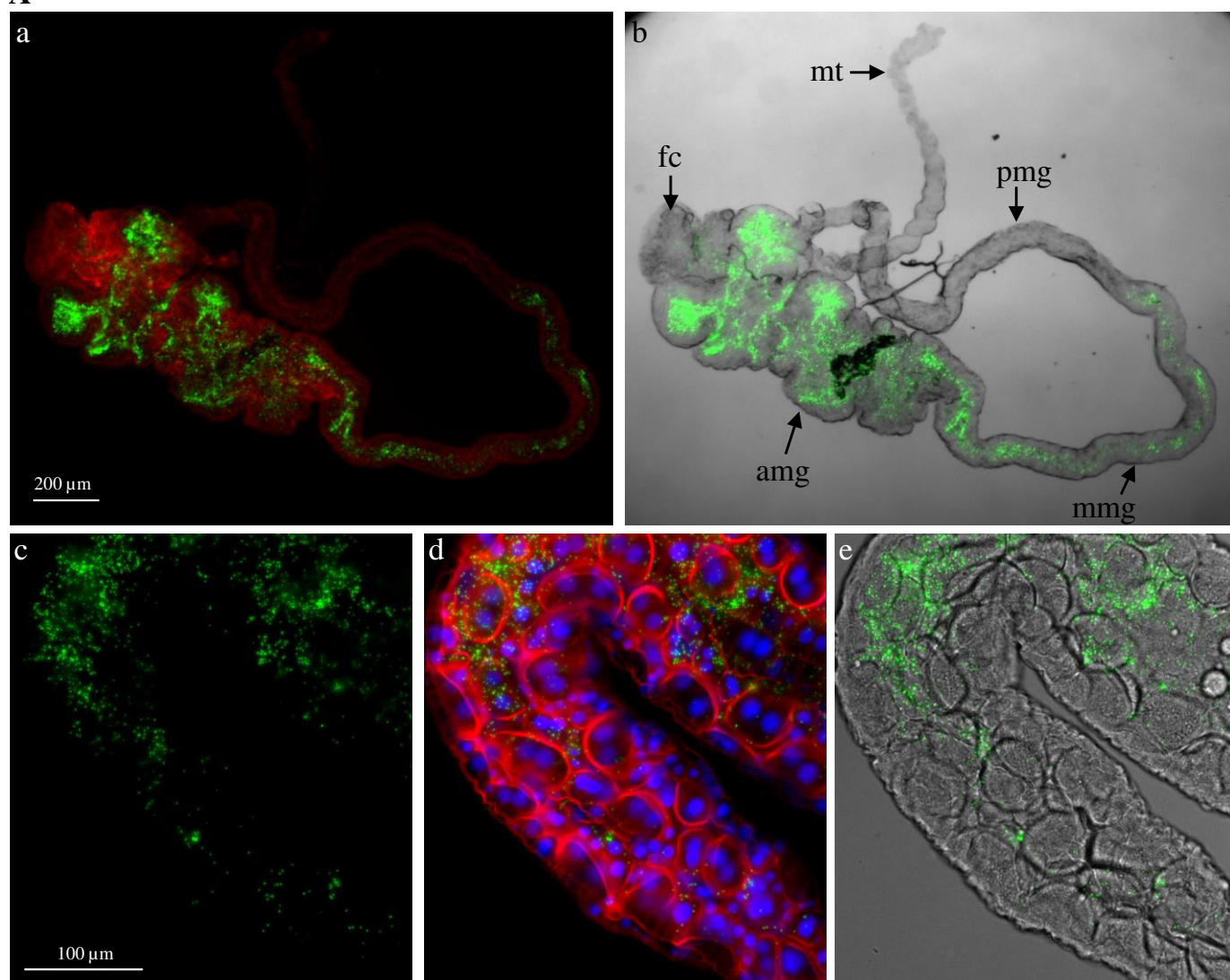
A



B



A



B

